



Published in final edited form as:

Shock. 2013 April ; 39(4): 336–342. doi:10.1097/SHK.0b013e31828d9324.

Complement C5a Generation by Staphylococcal Biofilms

Ashley E. Satorius², Jacob Szafranski², Derek Pyne², Mahesh Ghanesan³, Michael J. Solomon^{1,3}, Duane W. Newton⁴, David M. Bortz⁵, and John G. Younger^{1,2}

John G. Younger: jyounger@umich.edu

¹Biointerfaces Institute, University of Michigan, Ann Arbor, Michigan

²Departments of Emergency Medicine, University of Michigan, Ann Arbor, Michigan

³Chemical Engineering, University of Michigan, Ann Arbor, Michigan

⁴Clinical Microbiology Laboratory, Department of Pathology, University of Michigan, Ann Arbor, Michigan

⁵Department of Applied Mathematics, University of Colorado at Boulder, Boulder, Colorado

Abstract

Biofilms production is a central feature of nosocomial infection of catheters and other medical devices used in resuscitation and critical care. However, the very effective biofilm forming pathogen *Staphylococcus epidermidis* often produces a modest host inflammatory response and few of the signs and symptoms associated with more virulent pathogens. To examine the impact of bacterial biofilm formation on provocation of an innate immune response, we studied the elaboration of the major complement anaphylatoxin C5a by human serum upon contact with *S. epidermidis* biofilms. Wildtype *S. epidermidis* and mutants of *sarA* (a regulatory protein that promotes synthesis of the biofilm-forming polysaccharide intercellular adhesin, PIA) and *icaB* (responsible for post-export processing of PIA) were studied. C5a release, as a function of exposed biofilm surface area, was on the order of $1 \text{ fmol cm}^{-2} \text{ sec}^{-1}$ and was dependent on the presence of PIA. Experimental results were used to inform a physiologically-based pharmacokinetic model of C5a release by an infected central venous catheter, one of *S. epidermidis*' primary means of causing human disease. These simulations revealed that the magnitude of C5a release on a superior vena cava catheter completely covered with *S. epidermidis* would be lower than necessary to alert circulating leukocytes. Combined, the experimental and computational results are highly consistent with clinical observations in which the clinical signs of central line associated bloodstream infection are often muted in association with this important pathogen.

Correspondence to: John G. Younger, jyounger@umich.edu.

John G. Younger: Department of Emergency Medicine, 2800 Plymouth Road, North Campus Research Complex, Building 26, Room #329N, Ann Arbor, MI 48109, Phone: 734 647 7564

Publisher's Disclaimer: This is a PDF file of an unedited manuscript that has been accepted for publication. As a service to our customers we are providing this early version of the manuscript. The manuscript will undergo copyediting, typesetting, and review of the resulting proof before it is published in its final citable form. Please note that during the production process errors may be discovered which could affect the content, and all legal disclaimers that apply to the journal pertain.

Introduction

Resuscitation and ongoing care of critically ill and injured patients is unimaginable without the use of intravascular catheters, endotracheal tubes, and numerous other invasive medical devices. While life-saving, implanted artificial materials unavoidably carry the risk of bacterial contamination, infection, and harm. *Staphylococcus epidermidis* is an important cause of nosocomial infection and is the most-often identified pathogen associated with medical devices (13). Compared to many other clinically important bacterial pathogens, *S. epidermidis* is not particularly virulent in the traditional sense. Rather, its capacity to cause disease in critically ill patients is largely attributable to its tendency to produce tenacious biofilms on artificial surfaces (11). Clearance of this complex biomaterial is difficult if not impossible for host immune effectors, and the antibiotic resistance that biofilms confer on the bacteria they envelope often requires surgical removal and replacement of devices that become contaminated by this organism (6).

That staphylococcal biofilms are resistant to host defenses does not imply that they fail to activate brisk host response. In rodent models of infected subcutaneously-implanted biomaterials, inoculation with this organism produces an exuberant humoral and cellular inflammatory response (7, 16, 19). Of particular relevance to the current report are the recent observations that *S. epidermidis* biofilms activate the complement cascade but limit the deposition of complement C3b, thereby preventing effective killing by neutrophils (7). This biofilm feature was largely eliminated by deletion of the *ica* locus responsible for the synthesis, secretion, and post-secretion processing of the primary *S. epidermidis* extracellular polysaccharide, β -1,6-poly-N-acetyl glucosamine, also known as polysaccharide intercellular adhesin (PIA).

While interference of C3b deposition may limit opsonophagocytosis, it doesn't necessarily impair the production of anaphylatoxins during complement activation. C5a generation during serious infection is an important contributor to organ dysfunction and mortality in animal models of sepsis (1, 3, 15, 26, 27). In humans with severe sepsis, elevated circulating concentrations of C5a have been demonstrated at the time of initial hospital presentation (28). However, the immunology of C5a in the setting of more common but far less fulminant medical device infections is largely unstudied. In the current study, we have therefore examined human C5a production by contact with *S. epidermidis* biofilms. After establishing the relative contributions of the classical and alternative pathways to the activation of the complement cascade and generation of C5a against planktonic *S. epidermidis*, we examined the contribution of PIA to this response using both mutant strains with impaired PIA synthesis or extracellular display and with a novel assay presenting PIA as a complement target on the surface of agarose beads. Next, using previously described wild type organisms and their associated biofilm-deficient mutants, as well as with ten commensal skin isolates and ten isolates from bacteremic patients, we established a correlative relationship between the quantity of biofilm produced by a strain of *S. epidermidis* and the amount of C5a generated. Lastly, to place the amount of C5a elicited by staphylococcal biofilms in direct clinical context, we conducted a series of numerical simulations to explore the potential impact of a biofilm-coated central venous catheter on C5a concentrations in the vena caval and pulmonary microvascular circulation. Specifically, we addressed whether normal C5a

countermeasures, including dilution into large volumes of flowing blood, des-argylation by serum carboxypeptidases, and adsorption onto C5aR and C5L2 receptors on circulating leukocytes would be sufficient to functionally silence the plume of C5a leaving an infected device positioned in the human superior vena cava.

Methods

Ethics statement

The protocol for collecting isolates was approved by the University of Michigan Institutional Review Board, which deemed the work exempt. Blood isolates from bacteremic patients were provided to the group fully deidentified. For the collection of healthy control isolates, because neither human material nor clinical information was collected, written consent was not obtained. Organisms from the skin of healthy volunteers were immediately deidentified after verbal consent.

Bacterial strains and culture conditions

Staphylococcus epidermidis strains 1457 and an isogenic Δ icaB mutant were kindly provided by Michael Otto (24). Strain O-47 and an isogenic Δ sarA mutant likewise were provided by José R. Penadés (22). Skin commensal strains from ten healthy volunteers without recent hospitalization were collected from thumbprints on mannitol 4% NaCl agar plates. Ten clinical strains were isolated from blood cultures in which the organism was considered to be clinically significant. Clinical significance required that two or more cultures from anatomically distant blood draws recovered *S. epidermidis* of common colony morphology and identical metabolic and antibiotic resistance profiles (Vitek 2, BioMerieux). All skin and clinical isolates were confirmed as *S. epidermidis* by multiple locus genomic sequencing (see below).

Tryptic soy broth (TSB) supplemented with 1% glucose was used in all experiments. Planktonic cultures were grown at 37°C in a 1-cm orbit shaking incubator at 200 rpm. For experiments requiring biofilms, bacteria were grown planktonically for 6 hours, diluted to an OD (600nm) of 0.1, added to transferable solid phase 96 well plates (Nunc™ Thermo Scientific), and incubated without shaking for 48 hours at 37°C.(9) Biofilms were provided with fresh TSB 24 hours after inoculation. Successful seeding of transfer pegs was confirmed with scanning electron microscopy. Eighteen hours after inoculation, some pegs were removed and fixed in 4% glutaraldehyde. Samples were then progressively dehydrated through 50, 75, 90, 95, and 100% ethanol and dried under nitrogen gas. Prior to examination, each specimen sputter coated with gold (Polaron E5100, Quorum Technologies, West Sussex, UK). An Amray 1910 field emission gun scanning electron microscopy was used for imaging (Amray, Bedford, MA). Example scanning electron microscopy of this system during biofilm development is shown in Figure 1. Successful growth to surface confluence was confirmed with crystal violet staining (see below). Biofilm coated pegs were washed gently with phosphate-buffered saline (PBS) prior to use.

Differential light scattering for bacterial sizing

To establish the surface area of bacteria, the hydrodynamic radii of planktonic cells were determined using different light scattering as described elsewhere.(12) A compact goniometer fitted with a multi-tau digital correlator (ALV-GmbH, Langen, Germany) and 488 nm argon-ion laser (Innova 70C, Coherent, Santa Clara, CA) were used for scattering measurements as we have previously.(17) No significant differences between strains was noted (data not shown).

DNA sequencing for speciation and MLST

Genomic DNA was extracted using the Wizard® Genomic DNA Purification Kit (Promega, Madison, WI). PCR products were purified using PureLink™ PCR Purification Kit (Invitrogen™, Carlsbad, CA) and were sequenced using an Applied Biosystems Model 3730 XL sequencer. Chromatograms were analyzed using Sequencher™ 4.10.1 (Gene Codes Corporation, Ann Arbor, MI). For species confirmation, the 16S-23S rRNA intergenic spacer region was amplified using primers TCTACGAAGATGAGGGATA, forward, and TTTCCACCATATTTTGAATTGT, reverse. (2) For multilocus sequence typing 7 genes (*arc*, *aroE*, *gtr*, *mutS*, *pyr*, *tpiA*, and *yqiL*) were partially sequenced using the primers outlined elsewhere.(21) MLST types were then assigned to each strain using the online utility at www.sepidermidis.mlst.net.

C3b opsonization of planktonic cells and complement pathway analysis

Organisms were grown planktonically for 6 hours at 37°C, washed with PBS, and 10⁶ cells were incubated with 500 ul normal human serum (NS), C1q- or Factor B-depleted serum (Quidel, San Diego, CA), for 30 minutes at 37°C.(10, 29) Bound C3b was quantified flow-cytometrically using a FITC-labeled anti-C3b antibody (Thermo-Scientific, Fremont, CA). Cells opsonized with heat-inactivated serum served as a negative control. Extent of opsonization was normalized, for each strain, to the average mean channel fluorescence of normal serum.

PIA purification and PIA-lectin-bead generation

One liter batch cultures were grown for 24hours at 37°C and 60rpm shaking (Forma Incubated Shaker, Thermo Scientific). Purification of PIA was performed as in (14) with the following modifications. Following crude PIA collection from biofilm-bound cells, samples were passed over agarose-bound wheat-germ agglutinin (WGA) lectin beads (Vector Laboratories, Burlingame, CA) packed in 3mL tubes and equilibrated with 20mM Tris-HCl, 0.15M NaCl binding buffer. Bound EPS was eluted with 0.5M GlcNAc in 20mM Tris-HCl, 0.5M NaCl (pH=3.0) elution buffer.(25) Purified EPS was analyzed for molar mass distribution using a size exclusion chromatography column (Waters Ultrahydrogel 2000 and 250 columns connected in series) coupled to an online multi-angle laser light scattering device (Wyatt DAWN EOS MALLS device, GaAs 690nm laser) and refractive index detector (Wyatt OPTILAB DSP refractometric interferometer). The identity of PIA from column fractions was confirmed via affinity for WGA and by colorimetric assay for glucosamine. Fractions containing PIA were pooled and incubated with wheat-germ

agglutinin coated beads. Serum was exposed for 30 minutes to WGA-coated beads with or without PIA then assayed for C5a as above.

C5a production on biofilms

Biofilm-coated transferrable solid phase pegs were incubated for 45 minutes at 37°C with normal serum. C5a content was measured using a commercially available immunoassay (BD OptEIA™ Human C5a). Measured concentrations for each were expressed as flux from the biofilm surface (in moles $\text{cm}^{-2} \text{sec}^{-1}$) using the surface area of the serum-immersed portion of the peg as an assumed biofilm surface area. Biofilm content was quantified by submerging each peg in crystal violet for 15 minutes, washing three times in PBS, eluting the bound stain in 33% acetic acid, then measuring the eluent optical absorbance at 550nm.

Numerical analysis

Values used in simulating C5a elution from an infected central venous catheter are shown in Table 1. A central venous catheter with a biofilm-coated external surface was assumed to be positioned in the superior vena cava of a human adult. Venous blood flowing over the device mixed downstream into the right ventricle and was then ejected, fully mixed with blood from returning from the abdomen and lower extremities, into the pulmonary artery. C5a was assumed to leave the catheter surface at the flux noted in the above experiments and to subsequently dissipate in one of three ways. First, it underwent dilution first into the flow of the superior vena cava and then the entire right sided cardiac output. Second, it was subjected to des-arginylation via carboxypeptidase-N assuming Michaelis-Menten kinetics. Thirdly, it interacted with C5aR and C5L2 receptors on the surfaces of circulating leukocytes encountered during transit to the pulmonary microvasculature. Forward- and reverse binding constants for C5aR and C5L2 were not available. Therefore, values were modified from previously reported work with the fMLP receptor, which shares considerable functional and sequence homology with C5aR.(4) To adjust known fMLP rate constants to known equilibrium (K_D) measurements for C5aR and C5L2, we assumed the fMLP forward binding constant ($8.4 \times 10^7 \text{ M}^{-1}\text{sec}^{-1}$) across all receptors. The reverse constant was then adjusted to allow a K_D matching C5aR and C5L2 reported values. Sensitivity of pulmonary arterial C5a concentrations as a function of model parameters was performed as we have described elsewhere. (10) The model was built in Matlab 2011b/SimBiology 4.0 and numerical solutions were obtained using the SUNDIALS solver with default settings.

All statistical analyses were performed using the software environment R 2.13.2.(20) Comparisons between groups was performed with t-tests or analysis of variance where appropriate. In cases where initial F testing via ANOVA met statistical significance ($p < 0.01$), post-hoc comparisons were made with Tukey tests.

Results

Two common research strains of *S. epidermidis*, when grown planktonically, were readily opsonized by human complement as measured by anti-C3b flow cytometry (Figure 2, panels A and C). Depletion of either C1q or Factor B significantly reduced C3b deposition. Similarly, both pathways were found necessary for robust catalysis of C5 into C5a (Panels B

and D). The biofilm building block beta-1,6-N-acetyl-glucosamine polymer polysaccharide intercellular adhesin, or PIA, was also necessary for this interaction, in that deleting an intracellular protein necessary for optimal PIA synthesis (*sarA*), or deleting the extracellular deacetylase (*icaB*) involved in associating PIA with the bacterial surface significantly reduced C5a production. In these experiments, we measured C5a generation as flux (*i.e.*, the amount of protein produced per unit time per unit surface area). In this manner, direct comparisons between planktonic and biofilm activation could be made. Differential light scattering was used to establish the hydrodynamic radius and thus the surface area of planktonic cells. In this frame work, the production of C5a induced by a suspension of cells was very similar to the amount produced, per surface area, per unit time, of equivalent amount of biofilm surface area as discussed below. Neither the wild type nor mutant strains were killed by incubation with serum.

Using agarose beads functionalized with wheat germ agglutinin, we also examined the impact of surface display of PIA by an otherwise abiotic surface on C5a generation. PIA was purified from overnight biofilms using size exclusion chromatography and characterized with a combination of multi-angle laser light scattering and refractometry (Figure 3, panel A and B) then affixed to the surface of wheat germ agglutinin (WGA)-coated beads. Beads displaying PIA with an average molecular mass of 10^5 Dalton generated significantly more C5a than bare beads (Figure 3, panel C), indicating that this polymer is sufficient for complement activation when presented in a physically relevant manner.

To contrast the above planktonic experiments with the behavior of more clinically relevant artificial surface-infected conditions, biofilms were grown on pegs of known surface area immersed in media-filled microtiter wells. As with planktonic cells, deletion of either *sarA* or *icaB* significantly reduced elicited C5a during biofilm exposure (figure 4, panel A). Furthermore, there was excellent correlation between the amount of biofilm produced (as measured by crystal violet staining) and the amount of C5a generated under these defined conditions (figure 4, panel B, $p < 10^{-10}$, $R^2 = 0.75$). Inter-strain differences in C5a production between O-47 and 1457 corresponded to similar differences between strains when grown planktonically.

A comparable correlation was not seen between crystal violet-stainable biofilm and C5a production among 20 commensal skin and blood stream isolates. For ten strains collected from the skin of healthy volunteers and 10 recovered from the blood stream of patients in whom the isolate was clinically significant, there was no clear relationship between biofilm extent and C5a generation (figure 4, panel C, $p = 0.10$, $R^2 = 0.10$). Among these strains, we also examined the relationship between C5a generation and multilocus sequence type. No particular genotype was found to have greater capacity to elicit C5a (figure 4, panel D), suggesting altogether that in the clinical setting, determinants of C5a production are driven by features other than simply biofilm production.

Lastly, to consider the potential systemic importance of C5a production on a *S. epidermidis*-coated surface, we built a mathematical model of central venous line infection. C5a from a hypothetical catheter in the superior vena cava, producing C5a at the rate noted in our

experiments, was tracked through the superior vena cava, right heart, and pulmonary arterial tree (Figure 5, panel A). During this transit, the anaphylatoxin was diluted in flowing blood, degraded by serum carboxypeptidase-N, and adsorbed by leukocyte surface C5aR and C5L2 receptors according to kinetic parameters shown in Table 1. The model was built to address two questions. First, what is the fate of the plume of C5a leaving the catheter surface and are the concentrations of this signaling molecule in the downstream pulmonary vascular bed sufficient to activate intravascular leukocytes?

Figure 5, panel B shows modeled concentrations of C5a, C5a des arg, and leukocyte surface bound C5aR and C5L2 receptors in superior vena caval and pulmonary arterial blood in the setting of catheter infection using the biofilm-based flux estimates described above. In brief, the increase in concentration of C5a present in the pulmonary artery following a single pass over the infected device is 4-5 orders of magnitude smaller than the basal concentration of C5a des arg that has been noted in normal patients (28). To further place this in functional context, the C5a concentration to achieve 50%-maximum H₂O₂ production in murine neutrophils has been reported to be 100 nM; the concentration of free C5a predicted in the pulmonary arterial circulation in this model is 10 fM. Only 1/100,000th of the available C5aR and C5L2 receptors expected to be present in a patient with a peripheral white blood cell count of 5×10^6 mm³ were needed to quench the C5a produced by the catheter. To frame these results in a clearer context, in Figure 5, Panel C, these simulations were again performed, this time assuming that, in vivo, C5a production was 1,000-fold greater than our observations in vitro. Even in this case, C5a production was still predicted to be below the level of detection of cellular elements in the central circulation and pulmonary microvasculature.

Discussion

In the current work we describe factors promoting the production of human C5a following serum exposure to *S. epidermidis*. Both the classical and alternative pathways are necessary for full elaboration of the response, with depletion of C1q and the classical pathway more completely abolishing C5a production. Surface-displayed polysaccharide intercellular adhesion (β -1,6-poly-N-acetyl glucosamine) was also necessary for maximal C5a response. Reduction of PIA by altered expression or post-secretion processing limited anaphylatoxin production by both planktonic and biofilm-based cells, and display of PIA on agarose beads was sufficient to significantly increase C5a production compared to bare agarose surfaces. Importantly, our estimates for C5a generation at the biofilm surface, supported by numerical simulation, suggest that the degree of complement activation occurring in the venous circulation during a central line associated bloodstream infection would be expected to be insufficient to alert immune effector cells of the presence of nearby bacterial contamination.

Our observations extend significantly previously performed work in this area. (8) When other bacterial features remain fixed, changing the amount of biofilm formation by altering PIA production strongly affects the amount of C5a produced upon contact with serum. These observations, in conjunction with our results using planktonic bacteria, affirm a central role for the primary extracellular polysaccharide of this species in initiating a host inflammatory response. However, by further considering this relationship in 10 additional

commensal isolates and 10 strains recovered from patients with *S. epidermidis* bacteremia, it is apparent that the magnitude of biofilm formation is not the sole driver of complement activation. No significant correlation between biofilm formation and C5a production by these 20 wildtype strains was found, indicating that other activators, and potentially inhibitors, of the cascade are commonly present.

Because *S. epidermidis* very frequently causes disease by growing on the surfaces of implanted medical devices, and because the complement cascade is largely an enzymatic pathway that proceeds on the surface of cells or other materials with which it is presented, we endeavored in the current work to measure C5a generation as a flux, that is as the quantity of C5a produced on a contact surface as a function of both time and exposed area. In doing so, we believe we have moved measurement of complement interactions with individual cells and with biofilms onto more quantitative footing. This approach allowed us to exploit the extensive literature evaluating the biochemical details of various steps in the activation and deactivation of C5a. Specifically, our measurements in conjunction with previous characterization of enzyme and receptor kinetics in this pathway permitted us to make formal predictions of C5a behavior in the setting of an infected central venous catheter, one of *S. epidermidis*' most frequent clinical manifestations. While *in vitro* assays and *in vivo* model systems that examine foreign bodies in subcutaneous pockets or other relatively stagnant locations easily demonstrate complement-mediated effects, our simulations suggest this might not be true during intravascular device infections. The key difference between these two settings is the comparatively stagnant fluid flow in an abscess cavity compared to rapidly flowing blood passing by a catheter situated in the superior vena cava. Considering the fmol/cm²/sec flux values seen in our experimental system, and using blood flow, enzyme kinetic, and cell surface receptor binding kinetic values from the literature, it is apparent that local carboxypeptidase activity and the abundant C5aR and C5L2 receptor pools in the central circulation are more than sufficient to douse anaphylatoxin gradients within a few centimeters downstream of an infected catheter. While these simulations did not take into account ongoing recirculation of blood in an infected host, we nevertheless expect complement's contribution to any clinical manifestations of a central venous catheter infection with *S. epidermidis* to be very modest and possibly too small to detect. Some anaphylatoxin effects, such as cytoskeletal stiffening in activated neutrophils, which might serve to activate inflammatory cells sequestered in the pulmonary microvasculature were not considered. However, the concentrations of C5a predicted in our model are orders of magnitude below the 50% binding values for C5aR and C5L2, making signaling between an infected catheter and downstream tissue beds seem improbable. These theoretical findings are highly consistent with the clinically common occurrence of *S. epidermidis* being discovered incidentally to have formed a colonizing biofilm on an intravascular device of an otherwise unaffected patient. They are also in line with other recent work performed by our laboratory examining the impact of *S. epidermidis* extracellular polymeric substance and biofilm formation on C5a production at the single bacterium scale.(27) Only with ongoing refinement of quantitative analysis of the host-pathogen interface are such predictions possible. This work we believe lays a quantitative expectation of modest anaphylatoxin production by *S. epidermidis* in some clinical settings where it is commonly encountered.

Acknowledgments

This work was supported by grants through that National Institute for General Medical Sciences [grant numbers GM081702, GM069438] and the National Science Foundation [grant number Phys 0941227].

References

1. Flierl M, Perl M, Rittirsch D, Bartl C, Schreiber H, Fleig V, Schlaf G, Liener U, Brueckner U, Gebhard F, Huber-Lang M. The role of C5a in the innate immune response after experimental blunt chest trauma. *Shock*. 2008; 29:25–31. [PubMed: 17621257]
2. Forsman P, Tilsaia-Timisjarvi A, Alatosave T. Identification of staphylococcal and streptococcal causes of bovine mastitis using 16S-23S rRNA spacer regions. *Microbiology*. 1997; 143:3491–3500. [PubMed: 9387227]
3. Guo RF, Riedemann NC, Ward PA. Role of C5a-C5aR interaction in sepsis. *Shock*. 2004; 21:1–7. [PubMed: 14676676]
4. Hoffman JF, Keil ML, Riccobene TA, Omann GM, Linderman JJ. Interconverting receptor sites at 4°C for the neutrophil N-formyl peptide receptor. *Biochemistry*. 1996; 35:13047–13055. [PubMed: 8855940]
5. Hyun L, Whitfield P, Mackay C. Receptors for complement C5a. The importance of C5aR and the enigmatic role of C5L2. *Immunol Cell Bio*. 2008; 86:153–160. [PubMed: 18227853]
6. Karchmer AW, Longworth DL. Infections of intracardiac devices. *Cardiol Clin*. 2003; 21:253–271. vii. [PubMed: 12874897]
7. Kristian S, Birkenstock T, Sauder U, Mack D, Gotz F, Landmann R. Biofilm formation induces C3a release and protects *Staphylococcus epidermidis* from IgG and complement deposition and from neutrophil-dependent killing. *J Infect Dis*. 2008; 197:1028–1035. [PubMed: 18419540]
8. Kristian S, Birkenstock T, Sauder U, Mack D, Gotz F, Landmann R. Biofilm formation induces C3a release and protects *Staphylococcus epidermidis* from IgG and complement deposition and from neutrophil dependent killing. *J Inf Dis*. 2008; 197:1028–1035. [PubMed: 18419540]
9. Moskowitz S, Foster J, Emerson J, Burns J. Clinically feasible biofilm susceptibility assay for isolates of *Pseudomonas aeruginosa* from patients with cystic fibrosis. *J Clin Micro*. 2004; 42:1915–1922.
10. Nypaver CM, Thornton MM, Yin SM, Bracho DO, Nelson PW, Jones AE, Bortz DM, Younger DM. Dynamics of human complement-mediated killing of *Klebsiella pneumoniae*. *American Journal of Respiratory Cell and Molecular Biology*. 2010; 43:585–590. [PubMed: 20008281]
11. Otto M. *Staphylococcus epidermidis* -- the ‘accidental pathogen’. *Nature Reviews Microbiol*. 2009; 7:555–567.
12. Pecora, R. *Dynamic light scattering*. Plenum Press; New York, New York: 1985.
13. Rogers K, Fey P, Rupp M. Coagulase-negative staphylococcal infections. *Inf Dis Clin N Amer*. 2009; 23:73–98.
14. Sadvovskaya I, Vinogradov E, Flahaut S, Kogan G, Jabbouri S. Extracellular carbohydrate-containing polymers of a model biofilm-producing strain, *Staphylococcus epidermidis* RP62A. *Infection and Immunity*. 2005; 73:3007–3017. [PubMed: 15845508]
15. Schaeffer V, Cuschieri J, Garcia I, Knoll M, Billgren J, Jelacic S, Bulger E, Maier R. The priming effect of C5a on monocytes is predominantly mediated by the p38 MAPK pathway. *Shock*. 2007; 27:623–630. [PubMed: 17505301]
16. Schommer N, Christner M, Hentschke M, Ruckdeschel K, Aepfelbacher M, Rohder H. *Staphylococcus epidermidis* uses distinct mechanisms of biofilm formation to interfere with phagocytosis and activation of mouse macrophage-like cells 774A.1. *Infect Immunity*. 2011; 79:2267–2276. [PubMed: 21402760]
17. Shetty A, Solomon M. Aggregation in dilute solutions of high molar mass poly(ethylene) oxide and its effect on polymer turbulent drag reduction. *Polymer*. 2009; 50:261–270.
18. Skidgel R, Erdos E. Structure and function of human plasma carboxypeptidase N, the anaphylatoxin inactivator. *Int Immunopharmacol*. 2007; 7:1888–1899. [PubMed: 18039526]

19. Strunk T, Power Coombs M, Currie A, Richmond P, Golenbock D, Stoler-Barak L, Gallington L, Otto M, Burgner D, Levy O. TLR2 mediates recognition of live *Staphylococcus epidermidis* and clearance of bacteremia. *PLoS One*. 2010; 5:e101111. [PubMed: 20404927]
20. Team, R. D. C. R: A language and environment for statistical computing. R Foundation for Statistical Computing; Vienna: 2011.
21. Thomas J, Vargas M, Miragai M, Peacock S, Archer G, Enright M. Improved multilocus sequence typing scheme for *Staphylococcus epidermidis*. *J Clin Micro*. 2007; 45:616–619.
22. Tormo MA, Marti M, Valle J, Manna AC, Cheung AL, Lasa I, Penades JR. SarA is an essential positive regulator of *Staphylococcus epidermidis* biofilm development. *J Bacteriol*. 2005; 187:2348–2356. [PubMed: 15774878]
23. van Rossum A, Sprenger M, Visser F, Peels K, Valk J, JP R. An in vivo validation of quantitative blood flow imaging in arteries and veins using magnetic resonance phase shift techniques. *Euro Heart J*. 1991; 12:117–126.
24. Vuong C, Kocianova S, Voyich JM, Yao Y, Fischer ER, DeLeo FR, Otto M. A crucial role for exopolysaccharide modification in bacterial biofilm formation, immune evasion, and virulence. *J Biol Chem*. 2004; 279:54881–54886. [PubMed: 15501828]
25. Wang Y, Ao X, Vuong H, Konanur M, Miller F, Goodison S, Lubman D. Membrane glycoproteins associated with breast tumor cell progression identified by a lectin affinity approach. *J Proteome Res*. 2008; 7:4315–4325.
26. Ward PA. The dark side of C5a in sepsis. *Nature Rev Immunol*. 2004; 4:133–142. [PubMed: 15040586]
27. Xu D, Zaets S, Chen R, Lu Q, Rajan H, Yang X, Zhang J, Feketova E, Bogdan N, Deitch E, Cao Y. Elimination of C5aR prevents intestinal mucosal damage and attenuates neutrophil infiltration in local and remote organs. *Shock*. 2009; 31:493–499. [PubMed: 18791492]
28. Younger JG, Bracho DO, Chung-Esaki HM, Lee M, Rana GK, Sen A, Jones AE. Complement activation in emergency department patients with severe sepsis. *Academic Emergency Medicine*. 2010; 17:353–359. [PubMed: 20370773]
29. Younger JG, Shankar-Sinha S, Mickiewicz M, Brinkman AS, Valencia GA, Sarma JV, Younkin EM, Standiford TJ, Zetoune FS, Ward PA. Murine complement interactions with *Pseudomonas aeruginosa* and their consequences during pneumonia. *American Journal of Respiratory Cell and Molecular Biology*. 2003; 29:432–438. [PubMed: 14500254]

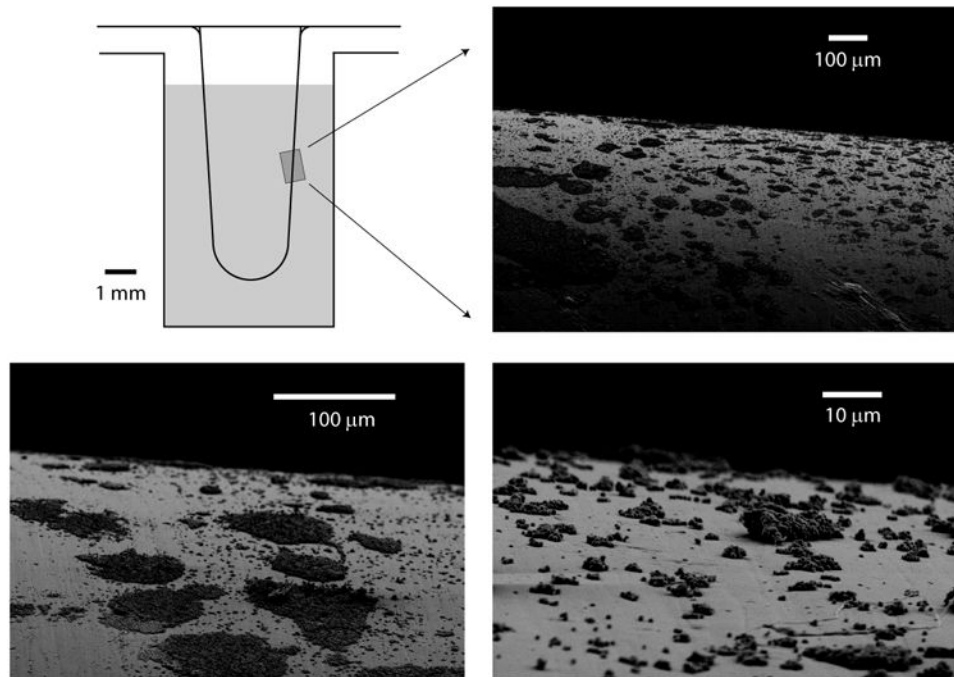


Figure 1. Solid phase system for growing *S. epidermidis* biofilms. Bacterial biofilms were cultivated on polycarbonate pegs immersed in bacterial growth media in a 96-well microtiter format as at upper left. Shown here are representative scanning electron micrographs of this process 18 hours after inoculation, where patches of biofilm are beginning to become confluent on the plastic surface. For experiments in this work, biofilms were provided with fresh media at this stage of growth and allowed to grow for a total of 48 hours prior to use. At that time, confluence was confirmed using crystal violet staining (see test for details). Biofilm covered pegs were then transferred to microtiter plates containing fresh serum or other reagents for measurement of complement activation.

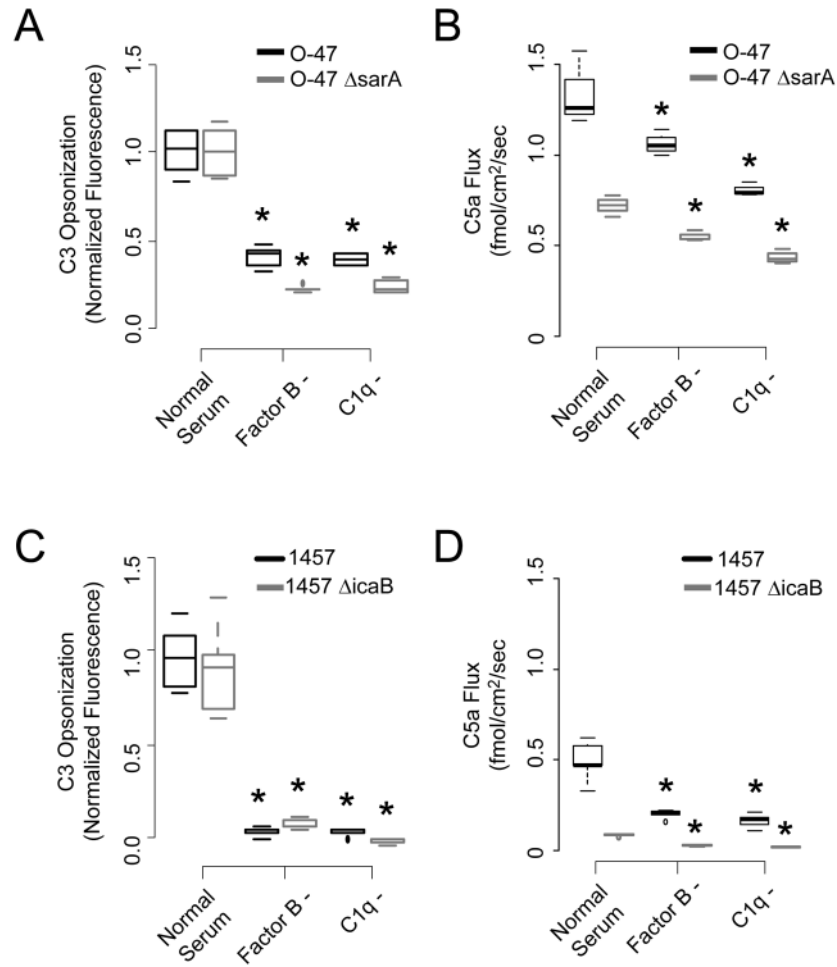


Figure 2.

Host and pathogen features affecting opsonization and C5a production in response to *S. epidermidis*. Panels A and C. Bacterial opsonization of wild type strains O-47 and 1457 and two mutants deficient in surface polysaccharide intercellular adhesin (Panel A, sarA, an alternate sigma factor necessary for full PIA production, and Panel C, icaB, an exo-deacetylase necessary for presentation of PIA on the bacterial surface). Opsonization was measured flow cytometrically against anti-C3b in normal serum and sera deficient in the alternative (Factor B-) and classical (C1q-) pathways. Boxplots represent 5th, 25th, 50th, 75th, and 95th percentile measurements, and asterisks mark statistical significance of p < 0.01 against normal serum. Panels B and D. Production of C5a upon serum exposure to planktonic O-47 and 1457 as a function of serum type. C5a production is displayed as flux of mediator from the bacterial surface in pmol/cm²/sec.

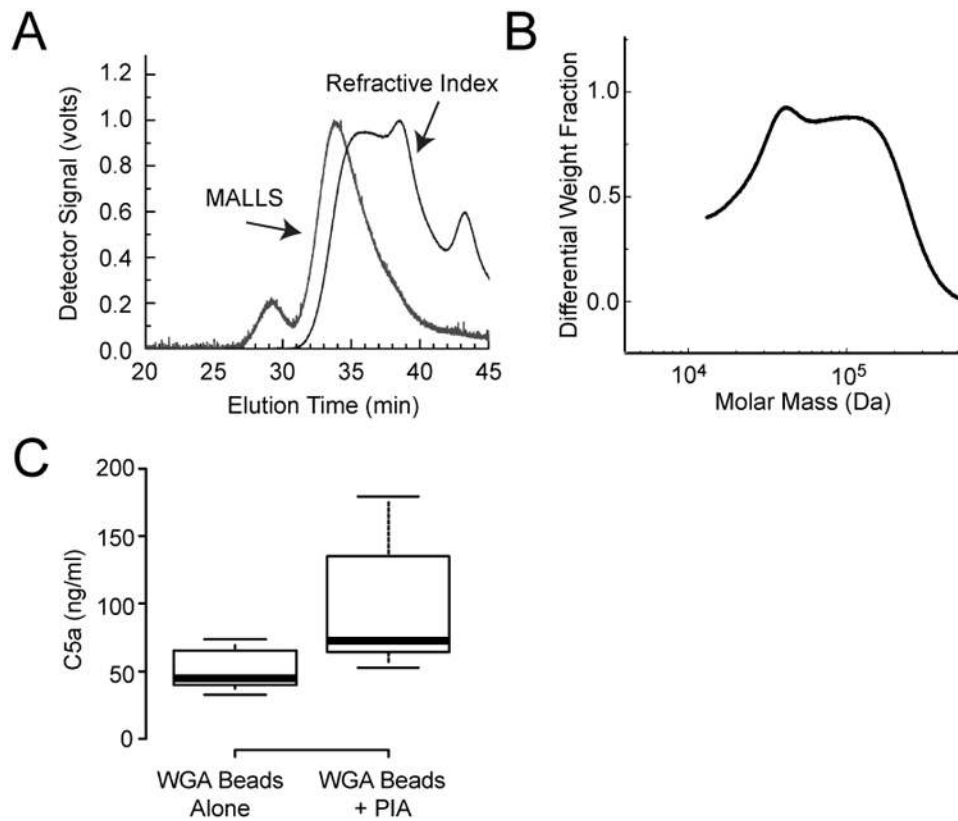


Figure 3. C5a production by abiotic surface-displayed polysaccharide intercellular adhesin. PIA was extracted from overnight biofilms and purified by size exclusion chromatography. The polysaccharide Panel A: SEC elution curve. Panel B: Estimated molar mass distribution of PIA recovered in Panel A. Panel C: C5a production by serum in contact with agarose beads functionalized with wheat germ agglutinin (WGA) alone and with attached PIA. Results are shown as 5th, 25th, 50th, 75th, and 95th %ile, $p < 0.05$.

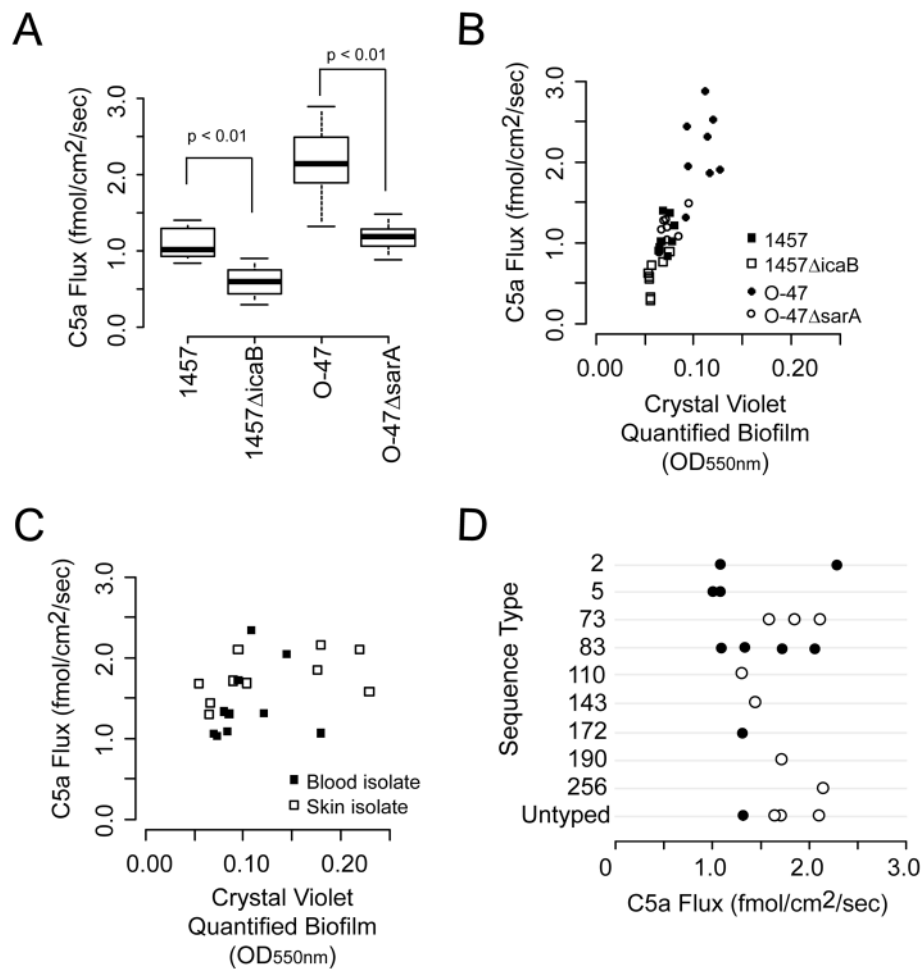


Figure 4.

C5a production by *S. epidermidis* biofilms. **A.** C5a flux (rate of elution off of the biofilm surface in fmol/cm²/sec) of 24-hr biofilms of two wildtype strains (1457 and O-47) and two mutants with impaired biofilm synthesis (*icaB*, which cannot deacetylate PIA and therefore loses it upon secretion into the environment, and *sarA*, which lacks an alternative sigma factor involved in PIA upregulation). Data reported as 5th, 25th, 50th, 75th, and 95th %ile. **B.** Flux as a function of total biofilm production of these four strains, as measured with crystal violet staining. The overall R² value for a linear fit of these data suggests 65% of variability in C5a flux can be explained by variation in biofilm formation (p < 0.001). **C.** C5a flux for biofilms formed by 10 isolates of *S. epidermidis* from healthy volunteers and 10 clinical blood culture isolates. Correlation between biofilm production and C5a flux was far less in these less-well-defined isolates. **D.** C5a flux for these 20 strains as a function of multilocus sequence type (MLST). Open circles – skin isolates; closed circles – blood isolates. Detailed strain lineage information did not predict the amount of C5a flux.

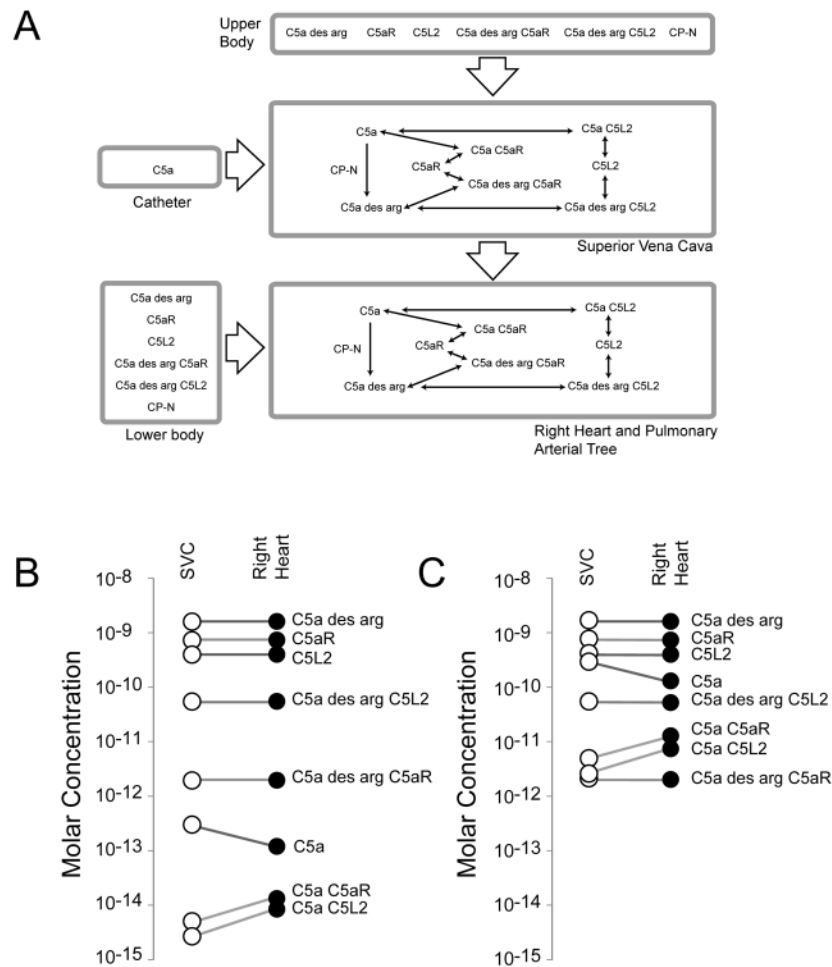


Figure 5. Predicted impact of C5a production in the setting of an infected central venous catheter. Panel A: A multicompartment physiologically-based pharmacokinetic model of an infected device positioned in the superior vena cave is shown. Large open block arrows indicate bulk blood flow between compartments. Panel B. Using experimental measurements of biofilm-induced C5a production and model assumptions shown in table 1, the concentrations of C5a, C5a des arg, and various species of C5a receptor states were modeled. In brief, our biofilm experiments suggest that a fully biofilm-coated central venous catheter would produce undetectably small amounts of C5a in blood in the central circulation, with carboxypeptidase degradation and receptor uptake keeping C5a levels very low. Panel C. Similar modeling result, using the higher levels of C5a production noted in our planktonic experiments. Even in the case of ~1,000-fold higher C5a production seen in these experiments, predicted levels of C5a would be below the level of detection, and far below the levels needed to induce significant cellular responses in leukocytes. See text for detail.

Table 1
Values used in numerical analysis

| Feature | Value | Reference |
|---|---|--|
| Intravascular catheter surface area | 5.4 cm ² | www.cookmedical.com |
| Superior vena caval blood flow | 0.041 liter sec ⁻¹ | (23) |
| Cardiac output | 0.083 liter sec ⁻¹ | (23) |
| Blood leukocyte concentration | 5.0 × 10 ⁹ liter ⁻¹ | |
| Hematocrit | 0.45 | |
| Surface-displayed C5aR per leukocyte | | |
| Surface-displayed C5L2 per leukocyte | | |
| K _D , C5a to C5aR | 3.5 nM | (5) |
| <i>k_f</i> | 8.4 × 10 ⁷ M ⁻¹ sec ⁻¹ | |
| <i>k_r</i> | 2.9 × 10 ⁻¹ sec ⁻¹ | |
| K _D , C5a des arg to C5aR | 600 nM | (5) |
| <i>k_f</i> | 8.4 × 10 ⁷ M ⁻¹ sec ⁻¹ | |
| <i>k_r</i> | 5.0 × 10 ¹ sec ⁻¹ | |
| K _D , C5a to C5L2 | 2.5 nM | (5) |
| <i>k_f</i> | 8.4 × 10 ⁷ M ⁻¹ sec ⁻¹ | |
| <i>k_r</i> | 2.1 × 10 ⁻¹ sec ⁻¹ | |
| K _D , C5a des arg to C5L2 | 12 nM | (5) |
| <i>k_f</i> | 8.4 × 10 ⁷ M ⁻¹ sec ⁻¹ | |
| <i>k_r</i> | 1.0 sec ⁻¹ | |
| K _M , carboxypeptidase-N for C5a | 260 uM | (18) |
| K _{cat} carboxypeptidase-N for C5a | 31 sec ⁻¹ | (18) |
| Basal plasma C5a des arg concentration | 1.6 nM | (28) |

C5aR: primary C5a receptor; C5L2: secondary C5a receptor